



UvA-DARE (Digital Academic Repository)

Curcumin reduces development of seizurelike events in the hippocampal-entorhinal cortex slice culture model for epileptogenesis

Drion, C.M.; Kooijman, L.; Aronica, E.; van Vliet, E.A.; Wadman, W.J.; Chameau, P.; Gorter, J.A.

DOI

[10.1111/epi.14667](https://doi.org/10.1111/epi.14667)

Publication date

2019

Document Version

Final published version

Published in

Epilepsia

License

Article 25fa Dutch Copyright Act

[Link to publication](#)

Citation for published version (APA):

Drion, C. M., Kooijman, L., Aronica, E., van Vliet, E. A., Wadman, W. J., Chameau, P., & Gorter, J. A. (2019). Curcumin reduces development of seizurelike events in the hippocampal-entorhinal cortex slice culture model for epileptogenesis. *Epilepsia*, *60*(4), 605-614. <https://doi.org/10.1111/epi.14667>

General rights



It is not permitted to download or to forward/distribute the text or part of it without the consent of the author(s) and/or copyright holder(s), other than for strictly personal, individual use, unless the work is under an open content license (like Creative Commons).

Disclaimer/Complaints regulations

If you believe that digital publication of certain material infringes any of your rights or (privacy) interests, please let the Library know, stating your reasons. In case of a legitimate complaint, the Library will make the material inaccessible and/or remove it from the website. Please Ask the Library: <https://uba.uva.nl/en/contact>, or a letter to: Library of the University of Amsterdam, Secretariat, Singel 425, 1012 WP Amsterdam, The Netherlands. You will be contacted as soon as possible.

UvA-DARE is a service provided by the library of the University of Amsterdam (<https://dare.uva.nl>)

Curcumin reduces development of seizurelike events in the hippocampal-entorhinal cortex slice culture model for epileptogenesis

Cato M. Drion¹  | Lieneke Kooijman¹ | Eleonora Aronica^{2,3} | Erwin A. van Vliet^{1,2}  | Wytse J. Wadman¹ | Pascal Chameau¹ | Jan A. Gorter¹

¹Center for Neuroscience, Swammerdam Institute for Life Sciences, University of Amsterdam, Amsterdam, The Netherlands

²Amsterdam UMC, University of Amsterdam, Department of (Neuro) Pathology, Amsterdam Neuroscience, Amsterdam, The Netherlands

³Stichting Epilepsie Instellingen Nederland (SEIN), The Netherlands

Correspondence

Jan A. Gorter, Center for Neuroscience, Swammerdam Institute for Life Sciences, University of Amsterdam, Amsterdam, The Netherlands.

Email: j.a.gorter@uva.nl

Funding information

Epilepsie Fonds, Grant/Award Number: EF 14-08; European Union's Seventh Framework Program (FP7, Epitarget), Grant/Award Number: 602102; EPISTOP, Grant/Award Number: 602391

Summary

Objective: Inhibition of the mammalian target of rapamycin (mTOR) pathway could be antiepileptogenic in temporal lobe epilepsy (TLE), possibly via anti-inflammatory actions. We studied effects of the mTOR inhibitor rapamycin and the anti-inflammatory compound curcumin—also reported to inhibit the mTOR pathway—on epileptogenesis and inflammation in an in vitro organotypic hippocampal-entorhinal cortex slice culture model.

Methods: Brain slices containing hippocampus and entorhinal cortex were obtained from 6-day-old rat pups and maintained in culture for up to 3 weeks. Rapamycin or curcumin was added to the culture medium from day 2 in vitro onward. Electrophysiological recordings revealed epileptiformlike activity that developed over 3 weeks.

Results: In week 3, spontaneous seizurelike events (SLEs) could be detected using whole cell recordings from CA1 principal neurons. The percentage of recorded CA1 neurons displaying SLEs was lower in curcumin-treated slice cultures compared to vehicle-treated slices (25.8% vs 72.5%), whereas rapamycin did not reduce SLE occurrence significantly (52%). Western blot for phosphorylated-S6 (pS6) and phosphorylated S6K confirmed that rapamycin inhibited the mTOR pathway, whereas curcumin only lowered pS6 expression at one phosphorylation site. Real-time quantitative polymerase chain reaction results indicated a trend toward lower expression of inflammatory markers IL-1 β and IL-6 and transforming growth factor β after 3 weeks of treatment with rapamycin and curcumin compared to vehicle.

Significance: Our results show that curcumin suppresses SLEs in the combined hippocampal-entorhinal cortex slice culture model and suggest that its antiepileptogenic effects should be further investigated in experimental models of TLE.

KEYWORDS

antiepileptogenesis, inflammation, mitogen-activated protein kinase, mammalian target of rapamycin, rat, seizurelike event

1 | INTRODUCTION

In recent years, studies have pointed toward a role for the mammalian target of rapamycin (mTOR) pathway in the development of temporal lobe epilepsy (TLE) after an initial insult.¹ Hyperactivation of the mTOR pathway, which is observed in patients with TLE, is thought to be proepileptogenic and accordingly, mTOR inhibition has been studied as an antiepileptogenic strategy.^{2–5} Rapamycin, a main inhibitor of the mTOR pathway, has been tested in several experimental models of TLE. Although antiepilept(ogen)ic effects of rapamycin have been reported in rodent models of TLE,^{6–9} it causes side effects after prolonged treatment.^{8,10,11}

In search of an alternative for rapamycin, we considered curcumin, the main component of the dietary spice turmeric, which comes from the root of the *Curcuma longa* plant. Curcumin was reported to inhibit the mTOR pathway.^{12–14} In addition, curcumin acts on the mitogen-activated protein kinase (MAPK) pathway¹⁵ and is anti-inflammatory^{13,16,17} and antioxidant.^{14,18} Inflammation is thought to play an important role in epileptogenesis,^{19–21} and oxidative stress is thought to contribute to epileptogenesis as well.^{22–25} Therefore, the anti-inflammatory and antioxidant properties of curcumin, combined with its ability to suppress the mTOR pathway, make it potentially antiepileptogenic. We set out to investigate effects of curcumin, compared to rapamycin, on epileptogenesis in the hippocampal-entorhinal network, *in vitro*.

The model we used is based on the organotypic hippocampal slice culture (OHSC) model.²⁶ OHSCs can be used to model epileptogenesis; the slicing of the brain tissue into 200–300- μm slices leads to the development of ictal activity after a couple of weeks *in vitro*. Recently, the model has been used for studying epileptogenesis as well as antiepileptic drug screening.^{27–29}

Here, we used organotypic slices containing both hippocampus and entorhinal cortex, the combined hippocampal-entorhinal cortex slice culture model,³⁰ to model TLE *in vitro* to compare antiepileptogenic actions of curcumin and rapamycin. We cultured hippocampal-entorhinal cortex slices for 3 weeks and studied effects of rapamycin and curcumin treatment on development of epilepticlike activity, electrophysiological properties of individual CA1 pyramidal neurons, the mTOR and MAPK pathways, and markers of inflammation and oxidative stress.

2 | MATERIALS AND METHODS

2.1 | Animals

Sprague Dawley rats (mother with pups; Envigo) were housed in a controlled environment ($21^{\circ}\text{C} \pm 2^{\circ}\text{C}$,

Key Points

- In the hippocampal-entorhinal cortex slice culture model, seizurelike activity progresses over time *in vitro*, resulting in SLEs after 3 weeks
- The occurrence of SLEs was reduced after treatment with curcumin ($10 \mu\text{mol}\cdot\text{L}^{-1}$), but not rapamycin ($20 \text{nmol}\cdot\text{L}^{-1}$), indicating antiepileptogenic effects of curcumin *in vitro*
- Antiepileptogenic effects of curcumin are possibly related to anti-inflammatory and antioxidant effects in combination with MAPK and (limited) mTOR inhibition

$55\% \pm 15\%$ humidity, 12 hours light/dark cycle with lights on from 08:00 AM to 8:00 PM) with water and food available *ad libitum*. Experiments were carried out according to European guidelines. Experimental protocols were approved by the Animal Welfare Committee according to Dutch law and in accordance with the European Communities Council Directive (2010/63/EU).

2.2 | Organotypic hippocampal-entorhinal cortex slice cultures

Organotypic slice cultures were prepared from Sprague Dawley rat pups (PND5/6; Envigo). Brains were dissected, embedded in 3% low melting point agarose (Merck) and sectioned in 300- μm -thick horizontal slices in cold ($2\text{--}4^{\circ}\text{C}$) Lonza buffer (L-15; Lonza) supplemented with glucose (sterile filtered, $10 \mu\text{mol}\cdot\text{L}^{-1}$ end concentration) and NaHCO_3 (sterile filtered, $5.8 \mu\text{mol}\cdot\text{L}^{-1}$ end concentration) using a VT1200S vibratome (Leica Biosystems). Slices containing ventral hippocampus and entorhinal cortex were dissected and plated onto cell culture inserts (Polyethylene Terephthalate $1.0 \mu\text{mol}\cdot\text{L}^{-1}$; BD Falcon; BD Biosciences) in 6-well plates (BD Falcon, BD Biosciences; 2–3 slices per well). The slice cultures were maintained in Neurobasal A culture medium (Thermo Fisher Scientific) supplemented with serum-free B27 (2%), GlutaMAX (0.25%) and gentamicin $10 \text{mg}/\text{mL}$ (0.3%; Thermo Fisher Scientific), and well plates were placed in a 5% CO_2 , 37°C incubator for up to 3 weeks. Medium was refreshed three times per week.

2.3 | Rapamycin and curcumin treatment

mTOR inhibitors rapamycin ($20 \text{nmol}\cdot\text{L}^{-1}$) and curcumin ($10 \mu\text{mol}\cdot\text{L}^{-1}$) were dissolved in dimethyl sulfoxide (DMSO; final concentration in the medium was 0.05%) and added to the culture medium from day 2 *in vitro* onward. The drug concentrations were chosen on the basis of previous studies

in slice cultures reporting effective mTOR inhibition by rapamycin³¹ or neuroprotective effects of curcumin.³² For vehicle treatment, 0.05% DMSO was added to the medium. Medium was refreshed three times per week.

2.4 | Whole cell patch-clamp and field potential recordings

Organotypic slice cultures were transferred into a recording chamber superfused with artificial cerebrospinal fluid (ACSF) containing (in mmol·L⁻¹) 120 NaCl, 3.5 KCl, 25 NaHCO₃, 10 D-glucose, 2.5 CaCl₂, 1.3 MgSO₄, 1.25 NaH₂PO₄ (extracellular chloride concentration; [Cl⁻]_{out} = 128.5 mmol·L⁻¹) and continuously bubbled with 95% O₂-5% CO₂ (pH = 7.4). Glass recording pipettes were pulled from borosilicate glass (Science Products) and had a resistance of 2-3 MΩ when filled with pipette solution (in mmol·L⁻¹): 131.25 potassium gluconate, 8.75 KCl, 0.5 ethyleneglycoltetraacetic acid, 10 hydroxyethylpiperazine ethane sulfonic acid, 4 Mg-adenosine triphosphate, 0.5 Na-guanosine triphosphate (intracellular chloride concentration; [Cl⁻]_i = 8.75 mmol·L⁻¹). Whole cell current and voltage clamp recordings were made at 32°C from the soma of CA1 pyramidal neurons. Recordings were made using an Axopatch 200B (Molecular Devices) and in-house software running under MATLAB (MathWorks). Signals were low-pass filtered at 5 kHz and sampled at 10 kHz. Series resistance ranged from 5 to 15 MΩ and was compensated to ~65%. Signals were corrected for liquid junction potential (+15 mV). Spontaneous postsynaptic currents (PSCs) were recorded at a holding potential of -85 mV, including both excitatory and inhibitory PSCs (reversal potential of excitatory PSC; E_{revExc} = 0 mV and reversal potential of inhibitory PSC; E_{revInh} = -70 mV). We also recorded at -50 mV, a voltage that allows discrimination between inhibitory (outward, positive) and excitatory (inward, negative) PSCs. In the current clamp configuration, a slow feedback system, guaranteed that current clamp recordings started at a defined membrane voltage of -70 mV. Field potential recordings were performed using glass pipettes filled with ACSF and a second Axopatch 200B amplifier in the current clamp mode.

Seizurelike events (SLEs) were observed and defined by visual inspection of recordings, using the characteristics described in previous work in OHSC.^{27,33} SLE-displaying CA1 neurons were detected in day in vitro (DIV) 21 slices, treated with either vehicle (n = 14 slices from five different culture experiments), rapamycin (n = 8 slices from three different culture experiments), or curcumin (n = 8 slices from four different culture experiments). On average, 2-4 cells were recorded per slice.

The analysis of the electrophysiological properties was performed using scripts written in MATLAB. The passive

properties were estimated from voltage responses evoked by 200-millisecond-duration hyperpolarizing current injections (10 pA). The membrane time constant (τ_m) and the input resistance (R_{in}) were determined by fitting the voltage response with a monoexponential function: $V(t) = I_{app} \times R_{in} \times e^{-t/\tau_m}$. Single action potential (AP) properties (threshold, amplitude, duration at half amplitude [half-width], after hyperpolarization amplitude) and repetitive AP firing properties were determined from voltage responses to 800-millisecond-duration depolarizing current injections ranging from 0 to 300 pA in 10-pA increments. AP firing properties were characterized by the mean spike frequency as a function of injected current.

2.5 | Western blot analysis

Western blot analysis was used to assess expression of phosphorylated S6 (pS6; mTOR activation), phosphorylated MAPK (pMAPK; MAPK activation), and vimentin (reactive astrocytes) in slices that were kept in culture for 1, 2, or 3 weeks. For each time point and treatment condition, 2-3 slices were pooled and stored in -80°C until use. Samples were homogenized in 50 μL lysis buffer (containing per 20 mL: 200 μL 1 mol·L⁻¹ Tris pH 8.0, 1 mL 3 mol·L⁻¹ NaCl, 2 mL 10% NP-40, 4 mL 50% glycerol, 800 μL Na-orthovanadate [10 mg/mL], 200 μL 0.5 mol·L⁻¹ EDTA, pH 8.0; 400 μL protease inhibitors, 200 μL 0.5 mol·L⁻¹ NaF and 11.2 mL H₂O). The protein concentration was determined using the bicinchoninic acid method.³⁴ Of each sample, 30 μg total protein was separated by sodium dodecyl sulfate polyacrylamide gel electrophoresis on a 12% gel. Subsequently, separated proteins were transferred onto polyvinylidene difluoride membranes (Immobilon-P, Merck) for 90 minutes at 100 V, using a wet electroblotting system (Bio-Rad Laboratories). Blots were blocked for 1 hour in 5% nonfat dry milk in Tris-buffered saline-Tween (TBS-T; 20 mmol·L⁻¹ Tris, 150 mmol·L⁻¹ NaCl, 0.1% Tween 20, pH 7.5). Blots were incubated overnight with primary antibody monoclonal rabbit anti-S6 (1:1000, 5G10; Cell Signaling Technology), monoclonal rabbit anti-phospho-S6 (Ser235/236, 1:1000, 91B2, Cell Signaling Technology), monoclonal rabbit anti-phospho-S6 (Ser240/244, 1:1000, D68F8, Cell Signaling Technology), monoclonal rabbit anti-phospho p44/42 MAPK (Erk1/2, 1:1500, D13.14.4E, Cell Signaling Technology), monoclonal rabbit anti-phospho-p70 S6 kinase (1:1000, 108D2, Cell Signaling Technology), monoclonal mouse antivimentin (1:1000, clone V9, M0725; Dako), monoclonal mouse anti-β-tubulin (1:50 000; Sigma), or monoclonal mouse anti-β-actin (1:5000, ACTN05 C4, Thermo Fisher Scientific). After several washes in TBS-T/5% nonfat dry milk, blots were incubated for 1 hour with secondary antibody horseradish

peroxidase (HRP)-labeled antirabbit (1:2500; Invitrogen), goat antirabbit HRP (1:2500, P0048, Dako), or goat anti-mouse IgG1 HRP (1:1000, 1070-05; Southern Biotech). After several washes in TBS-T, immunoreactivity was visualized using Pico Chemiluminescence substrate (Thermo Fisher Scientific). Expression of β -actin or tubulin was used as loading control. Chemiluminescent signal was detected using an ImageQuant LAS 4000 analyzer (GE Healthcare). Optical density of each band was measured using Photoshop CS5 (Adobe Systems). For each sample, the optical density of protein-of-interest bands was calculated relative to the optical density of reference-protein bands (all values were background corrected).

2.6 | Real-time quantitative polymerase chain reaction analysis

Slice cultures of 1, 2, and 3 weeks in vitro, treated with vehicle, rapamycin, or curcumin, were collected and stored in -80°C until further processing. For RNA isolation, slices were homogenized in Qiazol Lysis Reagent (Qiagen Benelux). Total RNA was isolated using the miRNeasyMini kit (Qiagen Benelux) according to the manufacturer's instructions. The concentration and purity of RNA were determined at 260/280 nm using a NanoDrop 2000 spectrophotometer (Thermo Fisher Scientific). To evaluate IL-1 β , IL-6, transforming growth factor β (TGF- β), and heme oxygenase (Hmox-1) mRNA expression, 300 ng of slice culture-derived total RNA was reverse-transcribed into cDNA using oligo dT primers. Quantitative polymerase chain reactions (qPCRs) were run on a LightCycler 480 thermocycler (Roche Applied Science) using the following primers: IL-1 β (forward: aaaaatgacctgtgtgtct, reverse: tcgttgctgtctctcctg), IL-6 (forward: gccagatcattcagagcaa, reverse: cattggaagtgggtagga), TGF- β (forward: cctggaagggtcaaac, reverse: cagttctctctgtggagctga), heme oxygenase-1 (forward: caacccaccaagttcaaca, reverse: aggcggtctagcctctctg). Quantification of data was performed using LinRegPCR software, in which linear regression on the log (fluorescence) per cycle number data is applied to determine the amplification efficiency per sample.³⁵ The starting concentration of each specific product was divided by the geometric mean of the starting concentration of the reference genes cyclophilin A (forward: cccacctgttcttcgacat, reverse: aaacagctcgaagcagc) and glyceraldehyde 3-phosphate dehydrogenase (forward: atgactctaccacggaag, reverse: tactcagcaccagcatcacc), and this ratio was compared between groups.

2.7 | Data analysis

For Western blot and real-time qPCR results, samples from at least 2-3 different experiments were used. Statistical analysis was done by nonparametrical testing (Kruskall-

Wallis followed by Dunn tests for multiple comparisons, or Mann-Whitney U tests), using Prism v5 (GraphPad Software). The analysis of the electrophysiological properties was performed using scripts written in MATLAB (see the section Whole Cell Patch-Clamp and Field Potential Recordings). T tests were used for statistical analysis unless otherwise stated.

Data are expressed as mean \pm SEM unless otherwise indicated. The number of observations is given in the figures or figure legends. A P value < 0.05 was assumed to indicate a significant difference.

3 | RESULTS

3.1 | Development of basic electrophysiological properties of CA1 neurons in hippocampal-entorhinal cortex slices over 3 weeks in vitro

First, we analyzed electrophysiological properties (passive properties and single AP properties) of CA1 pyramidal neurons of vehicle-treated slices during development over 3 weeks. Upon current injection, APs were recorded from CA1 pyramidal neurons in slices at DIV7 ($n = 41$), DIV14 ($n = 41$), and DIV21 ($n = 40$). Compared to DIV7, in slices of DIV14 and DIV21, neurons showed a decreased input resistance, membrane time constant, and AP threshold, and an increased AP amplitude. Neurons of DIV21 slices also displayed an increased capacitance and a decreased AP half-width, compared to DIV7. See Table 1 for the results. Average AP frequency in response to depolarizing current decreased over time in vitro; neurons of DIV21 slices ($n = 40$) and DIV14 slices ($n = 41$) had a decreased AP frequency in response to >60 pA injected current, compared to neurons of DIV7 ($n = 34-35$; two-way analysis of variance [ANOVA], for DIV $F = 526.3$, $P < 0.001$; Figure 1A).

3.2 | Repetitive AP firing properties of CA1 neurons in DIV21 hippocampal-entorhinal cortex slices treated with rapamycin, curcumin, or vehicle

When basic firing properties were compared between treatment conditions at DIV21, we found that neurons in curcumin-treated slices had a lower membrane time constant and a lower capacitance, but the AP frequency was not different, compared to neurons in vehicle-treated slices. Neurons in rapamycin-treated slices, however, displayed higher input resistance, AP half-width, and AP threshold, and lower AP amplitude at DIV21, compared to vehicle-treated slices (see Table 2 for the results). Furthermore, the average AP frequency in response to injected current was higher after rapamycin treatment,

TABLE 1 Basic firing properties (mean \pm SEM) of CA1 pyramidal neurons of vehicle-treated slice cultures of DIV7, DIV14, and DIV21

Vehicle	DIV7, n = 41	DIV14, n = 41	DIV21, n = 40
Input resistance, $M\Omega$	216 \pm 19	108 \pm 5 ^a	83 \pm 6 ^a
Membrane time constant, ms	15.41 \pm 0.97	10.46 \pm 1.11 ^a	9.40 \pm 0.96 ^a
Capacitance, pF	77.23 \pm 3.52	90.50 \pm 6.50	117.37 \pm 12.27 ^a
E rest, mV	-55.5 \pm 0.7	-55.4 \pm 1.0	-53.1 \pm 0.9
AP amplitude, mV	73.4 \pm 2.0	91.7 \pm 2.3 ^a	93.9 \pm 2.0 ^a
AP threshold, mV	-26.5 \pm 0.6	-29.8 \pm 0.6 ^a	-31.7 \pm 0.5 ^a
AP half-width, ms	2.15 \pm 0.12	1.94 \pm 0.16	1.50 \pm 0.11 ^a
AHP amplitude, mV	-8.03 \pm 0.74	-8.06 \pm 0.41	-7.80 \pm 0.58

AHP, after hyperpolarization; AP, action potential; DIV, day in vitro.
^a $P < 0.001$, unpaired *t* test, compared with DIV7.

compared to both curcumin- and vehicle-treated slices (two-way ANOVA, for treatment $F = 1129$, $P < 0.001$; Figure 1B).

3.3 | Development of seizurelike events in CA1 neurons in hippocampal-entorhinal cortex slices

Epileptogenesis in the slice cultures was electrophysiologically characterized by whole cell patch-clamp recordings of CA1 neurons. Spontaneous epilepticlike activity progressed over time (Figure 2A). At DIV7, slices showed inward currents of varying amplitudes. These inward currents developed into epilepticlike activity over time. At DIV21, SLEs occurred. SLEs, recorded in whole cell patch-clamp

recordings, were also reflected in field potential recordings (see Figure S1A).

The percentage of SLE-displaying cells was compared between vehicle-, rapamycin-, and curcumin-treated slices. Over all slices, the percentage of recorded CA1 neurons displaying SLEs was 72.5% (29/40) in vehicle-treated slices, 52% (13/25) in rapamycin-treated slices, and 25.8% (8/31) in curcumin-treated slices. As shown in Figure 2B and 2C, the percentage of SLE-displaying cells was significantly lower after curcumin treatment (Fisher's exact test; $P < 0.001$ compared to vehicle) but not after rapamycin treatment (Fisher's exact test; $P = 0.11$ compared to vehicle).

The average duration of SLEs was not different between vehicle-treated slices (140.6 \pm 16.4s, $n = 29$) and curcumin-treated slices (158.4 \pm 20.4s, $n = 8$), but significantly higher in rapamycin-treated slices (258.3 \pm 32.7s, $n = 13$, $P < 0.01$ compared to vehicle). Spontaneous excitatory postsynaptic current and spontaneous inhibitory postsynaptic current frequency distributions recorded at -50 mV (shown in Figure S1B) were not significantly different between the vehicle and curcumin conditions during interictal recordings.

3.4 | Effects of rapamycin and curcumin on the mTOR and MAPK pathways in hippocampal-entorhinal cortex slices

To investigate whether rapamycin and curcumin suppressed mTOR activation in hippocampal-entorhinal cortex slices, Western blot analysis was performed and the expression of pS6 was examined. Initially, DIV7, DIV14, and DIV21 slices treated with rapamycin and curcumin showed lower protein expression of pS6-Ser235/236 (Figure 3A). A Western blot for pS6-Ser240/244 (a different phosphorylation site on S6), however, showed that rapamycin-treated slices

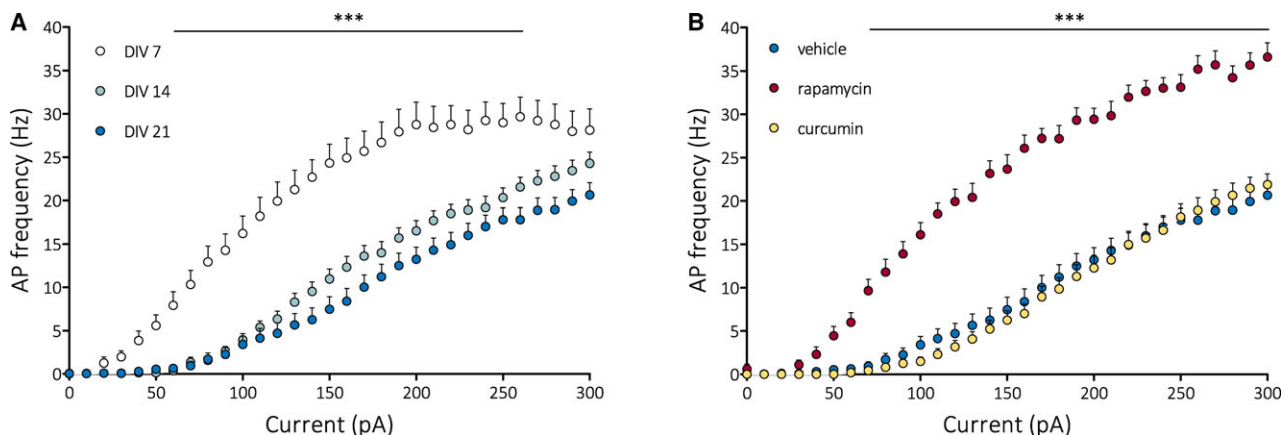


FIGURE 1 Action potential (AP; spike) frequency recorded in CA1 pyramidal neurons in response to current injections compared between (A) vehicle-treated slices at day in vitro (DIV) 7 ($n = 35$), DIV14 ($n = 41$), or DIV21 ($n = 40$) and (B) slice cultures of 21 DIV treated with vehicle ($n = 40$), rapamycin ($n = 25$), or curcumin ($n = 32$). *** $P < 0.001$ for DIV7, compared to DIV14 and DIV21 (A) or for rapamycin, compared to vehicle and curcumin (B)

TABLE 2 Basic firing properties (mean \pm SEM) of CA1 pyramidal neurons of slice cultures at DIV21 treated with vehicle, rapamycin, or curcumin

DIV21	Vehicle, n = 40	Rapamycin, n = 25	Curcumin, n = 31
Input resistance, M Ω	83 \pm 6	137 \pm 6 ^a	75 \pm 5
Membrane time constant, ms	9.40 \pm 0.96	11.55 \pm 1.20	6.50 \pm 0.88 ^b
Capacitance, pF	117.37 \pm 12.27	82.84 \pm 7.20 ^b	82.27 \pm 6.85 ^b
E rest, mV	-54.6 \pm 1.0	-56.0 \pm 1.3	-55.5 \pm 0.7
AP amplitude, mV	93.9 \pm 2.0	82.4 \pm 2.9 ^a	92.3 \pm 1.7
AP threshold, mV	-31.7 \pm 0.5	-29.6 \pm 0.6 ^b	-31.8 \pm 0.4
AP half-width, ms	1.50 \pm 0.11	1.94 \pm 0.20 ^b	1.65 \pm 0.07
AHP amplitude, mV	-7.80 \pm 0.58	-6.40 \pm 0.48	-7.29 \pm 0.48

AHP, after hyperpolarization; AP, action potential; DIV, day in vitro.

^a $P < 0.001$, ^b $P < 0.01$, unpaired *t* test, compared with vehicle.

($n = 3$), but not curcumin-treated slices ($n = 3$), showed a trend toward lower expression of pS6 compared to vehicle-treated slices ($n = 3$; Figure 3B). We then also tested phosphorylated S6K (p70-S6K) expression as additional readout of mTOR activation. S6K is the kinase that phosphorylates S6, downstream of mTOR. mTOR activates S6K through phosphorylation, so lower p70-S6K expression would indicate less mTOR activation (and would in turn lead to lower pS6 expression). Here too, only rapamycin-treated slices showed a trend toward lower expression of p70-S6K (Figure 3C). Western blot analysis for pMAPK revealed a trend toward suppression of the MAPK pathway by both rapamycin and curcumin (Figure 3D).

3.5 | Effects of rapamycin and curcumin on inflammation in hippocampal-entorhinal cortex slices

Immunohistochemistry (see Appendix S1) revealed an extensive amount of microglia and astrocytes with activated morphology in the hippocampal slices at DIV21 (see Figure S2). To quantify astrogliosis, we analyzed vimentin expression using Western blot analysis. The results indicated a trend that rapamycin-treated slices had higher expression of vimentin, whereas curcumin-treated slices had similar expression compared to vehicle-treated slices at DIV21 (Figure 3E). To further quantify the amount of inflammation, we studied gene expression of inflammatory markers IL-1 β , IL-6, and TGF- β , and to study oxidative stress, we tested gene expression of oxidative stress marker Hmox-1. Gene expression was compared between acute (DIV0) control slices ($n = 7$; IL-6: $n = 1$) and DIV21 slice cultures treated with vehicle ($n = 6$; IL-6: $n = 4$), rapamycin ($n = 6$; IL-6: $n = 2$), or curcumin ($n = 8$; IL-6: $n = 6$). For IL-1 β , IL-6, and TGF- β , a trend was present toward lower expression in rapamycin- and curcumin-treated slices, compared to vehicle-treated slices (Figure 4A-C). Hmox-1

expression was significantly higher in vehicle-treated slices, as shown by the normalized Hmox-1/GAPDH ratio, (15.3 ± 0.8 , $n = 6$) and in curcumin-treated slices (19.1 ± 2.1 , $n = 8$), but not in rapamycin-treated slices (8.3 ± 1.9 , $n = 6$), compared to control (0.7 ± 0.3 , $n = 7$; Kruskal-Wallis, 19.85, $P < 0.001$; Figure 4D).

4 | DISCUSSION

In the combined hippocampal-entorhinal cortex slice culture model, we found that occurrence of SLEs was reduced in curcumin-treated slices, but not in rapamycin-treated slices. These results suggest antiepileptogenic actions, which might be related to combined anti-inflammatory and antioxidant properties of curcumin in vitro. In the following paragraphs, we discuss this further.

First, we found that basic electrophysiological properties of CA1 neurons change over time in vitro in vehicle-treated slices. At 21 DIV, CA1 neurons of vehicle-treated slices show increased frequency adaptation, decreased input resistance and AP half-width, and an increased AP threshold. In rapamycin-treated slices, however, CA1 neurons showed less spike frequency adaptation, higher input resistance, and a lower AP threshold at 21 DIV. These characteristics are associated with immature neurons,³⁶ suggesting that neuronal maturation is slowed down by rapamycin in this model. This could be related to the findings that mTOR inhibitors such as rapamycin can reduce aging and promote longevity in mice.^{37,38}

Also, the reduced capacitance of CA1 neurons in rapamycin-treated slices suggested smaller cell size, which can be related to the role of mTOR in cell growth (reviewed in Saxton and Sabatini³⁹). Accordingly, rapamycin is known for inhibiting cell and body growth in rodent models.^{8,10,11}

Basic firing properties of CA1 neurons in curcumin-treated slices were not different from those observed in

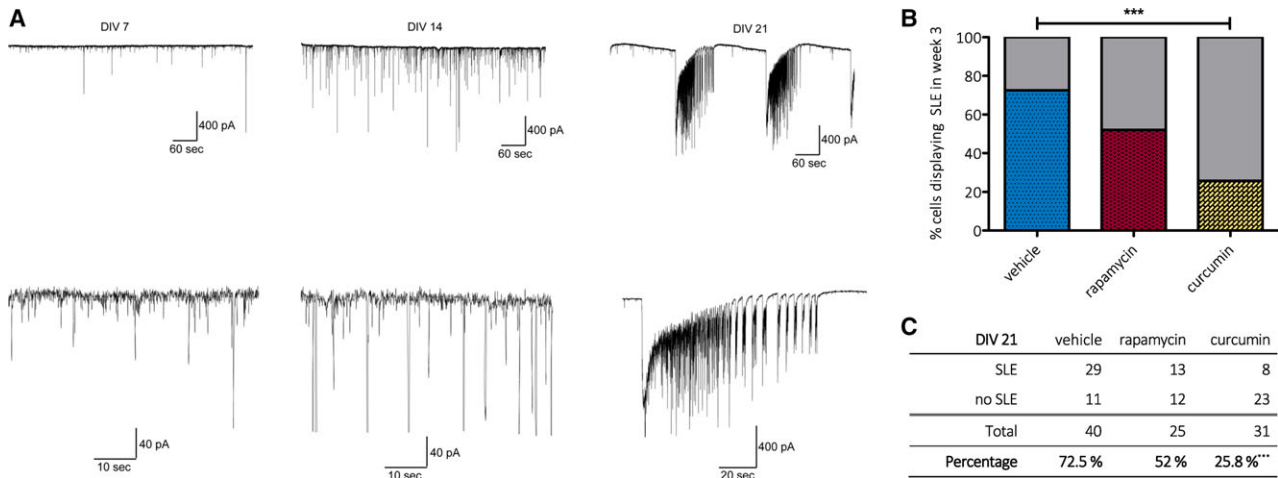


FIGURE 2 A, Upper traces show spontaneous inhibitory postsynaptic current/excitatory postsynaptic current activity recorded from CA1 neurons (V-hold was -85 mV) of vehicle-treated slices at day in vitro (DIV) 7, DIV14, and DIV21. The trace of DIV21 shows two seizurelike events (SLEs). Lower traces are magnifications of the upper traces. B, C, Quantification of the probability of SLEs occurring at DIV21 in vehicle-, rapamycin-, and curcumin-treated slices. *** $P < 0.001$ compared to vehicle

vehicle-treated slices, except for the capacitance, which was also lower after curcumin treatment. This could reflect mTOR-inhibiting properties of curcumin, in accordance with prior research.¹² However, our Western blot experiments suggest that curcumin, contrary to rapamycin, only reduced expression of pS6 Ser235-236 and not of pS6 240-244 and p70-S6K, which could indicate less effective mTOR inhibition by curcumin, compared to rapamycin.

In contrast to a previous study in which mTOR activity was related to epileptogenesis in OHSCs and where rapamycin had antiepileptogenic effects,³¹ we found that rapamycin enhanced excitability. This was also reflected in the SLE duration; SLEs in rapamycin-treated slices lasted longer, compared to vehicle and curcumin. An explanation for this enhanced excitability could be that rapamycin binds to the endoplasmic reticulum FK506-binding protein, increasing intracellular free calcium levels.⁴⁰ As we have replicated most of the culture conditions used by Berdichevsky et al.,³¹ we suggest that the difference could be related to our using combined hippocampus-entorhinal cortex slices, whereas they used hippocampus slices only, and possibly slight differences in timing.

Interestingly, curcumin effectively reduced SLE occurrence in our experiments, while showing less effective mTOR inhibition. In search of underlying mechanisms, we also studied MAPK activation, inflammation, and oxidative stress using Western blot analysis and qPCR. Western blot analysis of phosphorylated (p-)MAPK(ERK1/2) suggested a trend toward suppression of the MAPK pathway by both rapamycin and curcumin. Previous studies have suggested that curcumin can exert anti-inflammatory effects through MAPK inhibition.¹⁵⁻¹⁷

Inflammation plays an important role in temporal lobe epileptogenesis, and several pro-inflammatory mediators are thought to actively contribute to development of seizures via up-regulation of excitatory glutamatergic transmission and down-regulation of inhibitory γ -aminobutyric acidergic transmission.^{21,41}

The OHSC model allows for studying inflammatory mechanisms related to epileptogenesis. Coltman and Ide⁴² demonstrated activation of microglia and astrogliosis, which occur in response to the slicing-induced injury in OHSCs. Huuskonen et al.⁴³ showed the production of inflammatory markers IL-1 β , IL-6, and tumor necrosis factor α (TNF- α) by activated microglia and astrocytes in OHSCs over 3 weeks in vitro. Recently, it was illustrated that anti-inflammatory approaches can be antiepileptogenic in a study where epileptiform activity in OHSCs was reduced by applying anti-TNF- α polyclonal antibody to the slices.⁴⁴ However, another recent study reported no anti-epilept(ogen)ic effects of microglia depletion in OHSCs, suggesting that not all elements of the inflammatory response are essential for epileptogenesis in vitro.⁴⁵ In our experiments, increased expression of inflammatory markers IL-1 β , IL-6, and TGF- β was found in vehicle-treated slices at 21 DIV, and although the data did not reach significance at $P < 0.05$, a trend toward lower expression suggested a reduction by both rapamycin and curcumin. However, Western blot analysis for vimentin suggested a tendency of rapamycin to even further increase astrogliosis after 3 weeks of treatment, whereas curcumin slices showed comparable vimentin expression to vehicle slices. In addition to anti-inflammatory properties, curcumin also has antioxidant properties, which we studied through

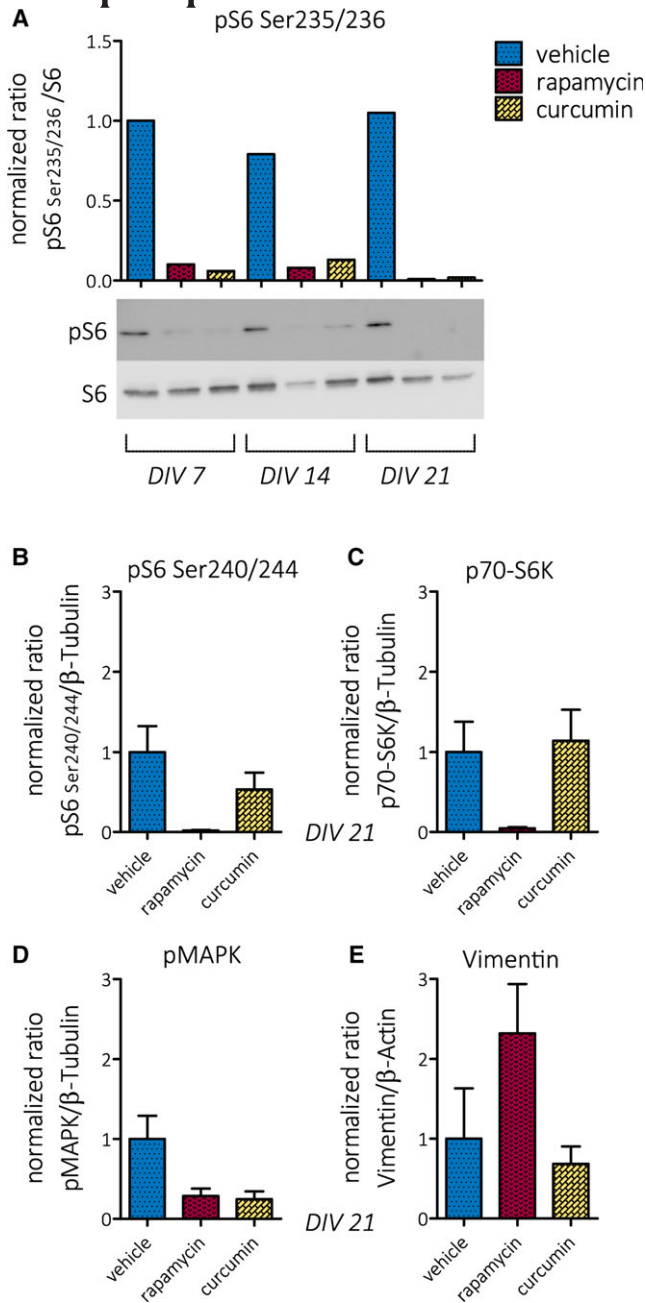


FIGURE 3 A, Western blot for phosphorylated S6 (pS6) Ser235/236 showing lower pS6/S6 ratios after rapamycin or curcumin treatment at day in vitro (DIV) 7, DIV14, and DIV21. B, Western blot for pS6 Ser240/244 showed a trend toward lower pS6 protein expression at DIV21 after rapamycin but not curcumin treatment, compared to vehicle ($n = 3$ for all treatment groups). C, Western blot for p70-S6K showed a trend toward lower p70-S6K protein expression at DIV21 after rapamycin but not curcumin treatment, compared to vehicle ($n = 3$ for all treatment groups). D, Western blot for phosphorylated mitogen-activated protein kinase (pMAPK) suggested a trend toward lower expression of pMAPK protein expression at DIV21 after rapamycin and curcumin treatment ($n = 3$ for vehicle and rapamycin, $n = 2$ for curcumin). E, Western blot for vimentin suggested a trend toward further higher vimentin protein expression in rapamycin-treated slices at DIV21, compared to vehicle and curcumin ($n = 3$ for vehicle and rapamycin, $n = 2$ for curcumin)

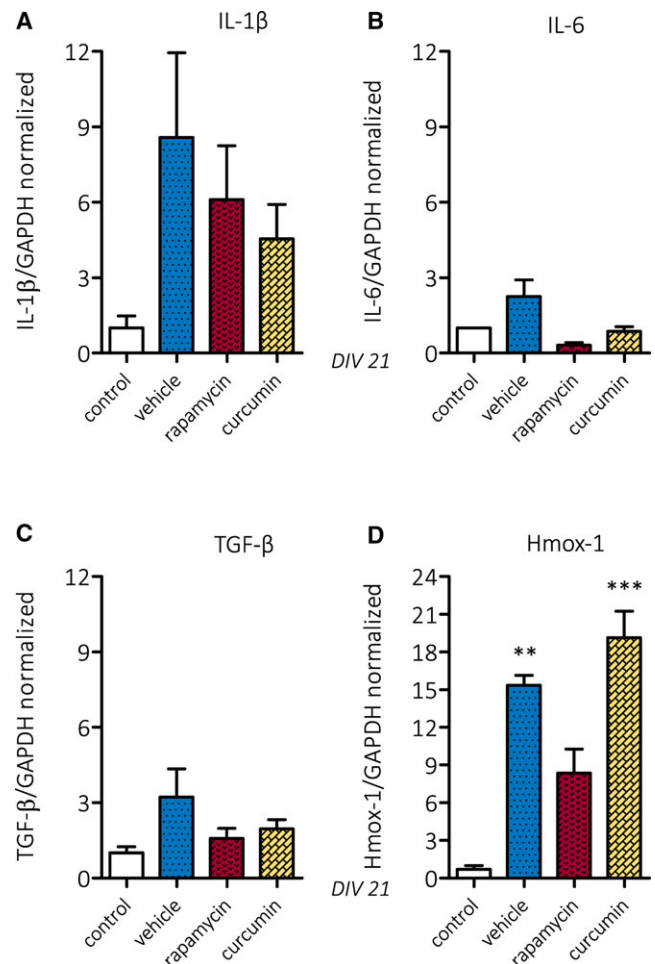


FIGURE 4 Real-time quantitative polymerase chain reaction (RT-qPCR) for inflammatory markers revealed a trend toward lower expression of (A) IL-1 β (B) IL-6, and (C) transforming growth factor β (TGF- β) after rapamycin and curcumin treatment, compared to vehicle, at day in vitro (DIV) 21. D, RT-qPCR for heme oxygenase (Hmox-1) showed that Hmox-1 expression was higher in vehicle- and curcumin-treated slices compared to controls at DIV21. Rapamycin-treated slices did not show higher expression of Hmox-1. Controls, $n = 7$ (IL-6, $n = 1$); vehicle, $n = 6$ (IL-6, $n = 4$); rapamycin, $n = 6$ (IL-6, $n = 2$); curcumin, $n = 8$ (IL-6, $n = 6$); samples from three different experiments. ** $P < 0.01$ and *** $P < 0.001$ compared to control

expression of Hmox-1 (an enzyme that is up-regulated in response to oxidative stress⁴⁶). Curcumin-treated slices displayed higher Hmox-1 expression compared to control, whereas rapamycin did not. Neither rapamycin nor curcumin suppressed formation of lactate dehydrogenase (LDH; see Figure S3).

Taken together, our results suggest that rapamycin was not able to suppress development of SLEs in this model, possibly because of inhibitory effects on neuronal maturation (reflected in electrophysiological characteristics), whereas curcumin suppressed SLE development without affecting basic electrophysiological properties of neurons. Curcumin was only partly effective as an mTOR inhibitor

and also showed trends toward MAPK inhibition, Hmox-1 up-regulation, and inhibition of inflammatory markers. In concert, these changes may provide antiepileptogenic actions, which should be further investigated in experimental animal models of epilepsy.

ACKNOWLEDGMENTS

The research leading to these results has received funding from the Dutch Epilepsy Foundation, project number EF 14-08 (C.M.D., J.A.G.) and the European Union's Seventh Framework Program (FP7/2007-2013) under grant agreements 602102 (EPITARGET; E.A., J.A.G., E.A.v.V.) and 602391 (EPISTOP; E.A.).

DISCLOSURE

None of the authors has any conflict of interest to disclose. We confirm that we have read the Journal's position on issues involved in ethical publication and affirm that this report is consistent with those guidelines.

ORCID

Cato M. Drion  <https://orcid.org/0000-0002-3926-3110>

Erwin A. van Vliet  <https://orcid.org/0000-0001-5747-3202>

REFERENCES

- Wong M. Mammalian target of rapamycin (mTOR) inhibition as a potential antiepileptogenic therapy: from tuberous sclerosis to common acquired epilepsies. *Epilepsia*. 2010;51:27–36.
- Galanopoulou AS, Gorter JA, Cepeda C. Finding a better drug for epilepsy: the mTOR pathway as an antiepileptogenic target. *Epilepsia*. 2012;53:1119–30.
- McDaniel SS, Wong M. Therapeutic role of mammalian target of rapamycin (mTOR) inhibition in preventing epileptogenesis. *Neurosci Lett*. 2011;497:231–9.
- Sadowski K, Kotulska-Jóźwiak K, Jóźwiak S. Role of mTOR inhibitors in epilepsy treatment. *Pharmacol Rep*. 2015;67:636–46.
- Switon K, Kotulska K, Janusz-Kaminska A, et al. Molecular neurobiology of mTOR. *Neuroscience*. 2017;341:112–53.
- Buckmaster PS, Ingram EA, Wen X. Inhibition of the mammalian target of rapamycin signaling pathway suppresses dentate granule cell axon sprouting in a rodent model of temporal lobe epilepsy. *J Neurosci*. 2009;29:8259–69.
- Huang X, Zhang H, Yang J, et al. Pharmacological inhibition of the mammalian target of rapamycin pathway suppresses acquired epilepsy. *Neurobiol Dis*. 2010;40:193–9.
- van Vliet EA, Forte G, Holtman L, et al. Inhibition of mammalian target of rapamycin reduces epileptogenesis and blood-brain barrier leakage but not microglia activation. *Epilepsia*. 2012;53:1254–63.
- Zeng L-H, Rensing NR, Wong M. The mammalian target of rapamycin signaling pathway mediates epileptogenesis in a model of temporal lobe epilepsy. *J Neurosci*. 2009;29:6964–72.
- Drion CM, Borm LE, Kooijman L, et al. Effects of rapamycin and curcumin treatment on the development of epilepsy after electrically induced status epilepticus in rats. *Epilepsia*. 2016;57:688–97.
- Sliwa A, Plucinska G, Bednarczyk J, et al. Post-treatment with rapamycin does not prevent epileptogenesis in the amygdala stimulation model of temporal lobe epilepsy. *Neurosci Lett*. 2012;509:105–9.
- Beevers CS, Chen L, Liu L, et al. Curcumin disrupts the mammalian target of rapamycin-raptor complex. *Cancer Res*. 2009;69:1000–8.
- Zhou H, Beevers CS, Huang S. Targets of curcumin. *Curr Drug Targets*. 2011;12:332–47.
- Maheshwari RK, Singh AK, Gaddipati J, et al. Multiple biological activities of curcumin: a short review. *Life Sci*. 2006;78:2081–7.
- Camacho-Barquero L, Villegas I, Sánchez-Calvo JM, et al. Curcumin, a Curcuma longa constituent, acts on MAPK p38 pathway modulating COX-2 and iNOS expression in chronic experimental colitis. *Int Immunopharmacol*. 2007;7:333–42.
- Kim G-Y, Kim K-H, Lee S-H, et al. Curcumin inhibits immunostimulatory function of dendritic cells: MAPKs and translocation of NF- κ B as potential targets. *J Immunol*. 2005;174:8116–24.
- Cho J-W, Lee K-S, Kim C-W. Curcumin attenuates the expression of IL-1 β , IL-6, and TNF- α as well as cyclin E in TNF- α -treated HaCaT cells; NF- κ B and MAPKs as potential upstream targets. *Int J Mol Med*. 2007;19:469–74.
- Parada E, Buendia I, Navarro E, et al. Microglial HO-1 induction by curcumin provides antioxidant, antineuroinflammatory, and glioprotective effects. *Mol Nutr Food Res*. 2015;59:1690–700.
- Aronica E, Bauer S, Bozzi Y, et al. Neuroinflammatory targets and treatments for epilepsy validated in experimental models. *Epilepsia*. 2017;58:27–38.
- Gorter JA, van Vliet EA, Aronica E. Status epilepticus, blood-brain barrier disruption, inflammation, and epileptogenesis. *Epilepsy Behav*. 2015;49:13–6.
- Vezzani A, French J, Bartfai T, et al. The role of inflammation in epilepsy. *Nat Rev Neurol*. 2011;7:31–40.
- Aguiar CCT, Almeida AB, Araújo PVP, et al. Oxidative stress and epilepsy: literature review. *Oxid Med Cell Longev*. 2012;2012:795259.
- Shin E-J, Jeong JH, Chung YH, et al. Role of oxidative stress in epileptic seizures. *Neurochem Int*. 2011;59:122–37.
- Pauletti A, Terrone G, Shekh-Ahmad T, et al. Targeting oxidative stress improves disease outcomes in a rat model of acquired epilepsy. *Brain*. 2017;140:1–15.
- Arena A, Zimmer TS, van Scheppingen J, et al. Oxidative stress and inflammation in a spectrum of epileptogenic cortical malformations: molecular insights into their interdependence. *Brain Pathol*. 2018 Oct 10 [Epub ahead of print].
- Stoppini L, Buchs PA, Muller D. A simple method for organotypic cultures of nervous tissue. *J Neurosci Methods*. 1991;37:173–82.
- Dyhrfeld-Johnsen J, Berdichevsky Y, Swiercz W, et al. Interictal spikes precede ictal discharges in an organotypic hippocampal slice culture model of epileptogenesis. *J Clin Neurophysiol*. 2010;27:418–24.

28. Berdichevsky Y, Dzhala V, Mail M, et al. Interictal spikes, seizures and ictal cell death are not necessary for post-traumatic epileptogenesis in vitro. *Neurobiol Dis*. 2012;45:774–85.
29. Wong M. Epilepsy in a dish: an in vitro model of epileptogenesis. *Epilepsy Curr*. 2011;11:153–4.
30. Wahab A, Albus K, Heinemann U. Age- and region-specific effects of anticonvulsants and bumetanide on 4-aminopyridine-induced seizure-like events in immature rat hippocampal-entorhinal cortex slices. *Epilepsia*. 2011;52:94–103.
31. Berdichevsky Y, Dryer AM, Saponjian Y, et al. PI3K-Akt signaling activates mTOR-mediated epileptogenesis in organotypic hippocampal culture model of post-traumatic epilepsy. *J Neurosci*. 2013;33:9056–67.
32. Hoppe JB, Haag M, Whalley BJ, et al. Curcumin protects organotypic hippocampal slice cultures from A β 1–42-induced synaptic toxicity. *Toxicol In Vitro*. 2013;27:2325–30.
33. Dreier JP, Heinemann U. Late low magnesium-induced epileptiform activity in rat entorhinal cortex slices becomes insensitive to the anticonvulsant valproic acid. *Neurosci Lett*. 1990;119:68–70.
34. Smith PK, Krohn RI, Hermanson GT, et al. Measurement of protein using bicinchoninic acid. *Anal Biochem*. 1985;150:76–85.
35. Ruijter JM, Ramakers C, Hoogaars WMH, et al. Amplification efficiency: linking baseline and bias in the analysis of quantitative PCR data. *Nucleic Acids Res*. 2009;37:e45.
36. Spigelman I, Zhang L, Carlen PL. Patch-clamp study of postnatal development of CA1 neurons in rat hippocampal slices: membrane excitability and K⁺ currents. *J Neurophysiol*. 1992;68:55–69.
37. Wilkinson JE, Burmeister L, Brooks SV, et al. Rapamycin slows aging in mice. *Aging Cell*. 2012;11:675–82.
38. Miller RA, Harrison DE, Astle CM, et al. Rapamycin-mediated lifespan increase in mice is dose and sex dependent and metabolically distinct from dietary restriction. *Aging Cell*. 2014;13:468–77.
39. Saxton RA, Sabatini DM. mTOR Signaling in growth, metabolism, and disease. *Cell*. 2017;168:960–76.
40. Hoeffler CA, Tang W, Wong H, et al. Removal of FKBP12 enhances mTOR-raptor interactions, LTP, memory, and perseverative/repetitive behavior. *Neuron*. 2008;60:832–45.
41. Vezzani A, Aronica E, Mazarati A, et al. Epilepsy and brain inflammation. *Exp Neurol*. 2013;244:11–21.
42. Coltman BW, Ide CF. Temporal characterization of microglia, IL-1 β -like immunoreactivity and astrocytes in the dentate gyrus of hippocampal organotypic slice cultures. *Int J Dev Neurosci*. 1996;14:707–19.
43. Huuskonen J, Suuronen T, Miettinen R, et al. A refined in vitro model to study inflammatory responses in organotypic membrane culture of postnatal rat hippocampal slices. *J Neuroinflammation*. 2005;2:2–25.
44. Chong SA, Balosso S, Vandenplas C, et al. Intrinsic inflammation is a potential anti-epileptogenic target in the organotypic hippocampal slice model. *Neurotherapeutics*. 2018;15:470–88.
45. Park K, Dzhala V, Saponjian Y, et al. What elements of the inflammatory system are necessary for epileptogenesis in vitro? *eNeuro*. 2015;2:1–12.
46. Motterlini R, Foresti R, Bassi R, et al. Curcumin, an antioxidant and anti-inflammatory agent, induces heme oxygenase-1 and protects endothelial cells against oxidative stress. *Free Radic Biol Med*. 2000;28:1303–12.

SUPPORTING INFORMATION

Additional supporting information may be found online in the Supporting Information section at the end of the article.

How to cite this article: Drion CM, Kooijman L, Aronica E, et al. Curcumin reduces development of seizurelike events in the hippocampal-entorhinal cortex slice culture model for epileptogenesis. *Epilepsia*. 2019;60:605–614. <https://doi.org/10.1111/epi.14667>